Optical add–drop multiplexers based on the antisymmetric waveguide Bragg grating

Jose M. Castro, David F. Geraghty, Seppo Honkanen, Christoph M. Greiner, Dmitri Iazikov, and Thomas W. Mossberg

A novel optical add–drop multiplexer (OADM) based on a null coupler with an antisymmetric grating was designed and experimentally demonstrated. The antisymmetric grating exclusively produces a reflection with mode conversion in a two-mode waveguide. This improves the performance compared with previous demonstrations that used tilted Bragg gratings. Our design minimizes noise and cross talk produced by reflection without mode conversion. In addition, operational bandwidth and, versatility are improved while the compactness and simplicity of the null coupler OADM are maintained. © 2006 Optical Society of America

OCIS codes: 130.3120, 060.2330, 130.1750, 230.1480.

1. Introduction

Simple elements to enable the integration of optical devices are required for further development of all-optical networks. Key functions such as filtering and multiplexing have already been demonstrated optically by use of bulk elements such as fiber Bragg gratings and circulators.[1] Devices that use tilted Bragg gratings (TBGs) and asymmetric Y branches[2–4] represent a step toward optical integration because they can be implemented in optical chips without the need for external circulators. These devices are based on the mode-conversion properties of TBGs and the mode-splitting characteristics of an asymmetric Y branch. They can filter an incoming signal and direct the result of the processing to a desired port. However, TBGs produce multiple reflections, only one of which provides the desired mode conversion.[5–7] The unwanted reflections produce noise, cross talk, and backreflection, and they place stringent requirements on the performance of the Y branch.

J. M. Castro (jmcastro@e-mail.arizona.edu), D. F. Geraghty, and S. Honkanen are with the University of Arizona. J. M. Castro and D. F. Geraghty are with the Department of Electrical and Computer Engineering, 1230 East Speedway Avenue, Tucson, Arizona 85721-0104. S. Honkanen is with the College of Optical Sciences, 1630 East University Boulevard, Tucson, Arizona, 85721. C. M. Greiner, D. Iazikov, and T. W. Mossberg are with LightSmyth Technologies, Inc., Suite 250 860 West Park Street, Eugene, Oregon 97401.

Received 24 June 2005; accepted 9 September 2005.
0003-6935/06/061236-08$15.00/0
© 2006 Optical Society of America

Schemes to produce only the desired reflection with mode conversion were proposed recently that used Bragg gratings in an asymmetric configuration.[8–11] Experimental attempts to implement these schemes have required difficult fabrication and alignment techniques; although the unwanted reflections were reduced, they were still strong, with approximately 90% of the input power still reflected.[10]

In this paper we show the design and experimental results of a novel optical add–drop multiplexer (OADM) fabricated with an antisymmetric waveguide Bragg grating.[11] Modeling[11,12] and recent experimental demonstrations[13,14] of this grating show that reflection with mode conversion in a two-mode waveguide can be achieved without the spurious reflections produced by the TBGs.

Our design is based on coupled-mode theory applied to reflective gratings[15] and beam propagation simulations.[16] These techniques have shown excellent agreement with experimental results when they were applied to a similar OADM based on a TBG.[6] Prototypes for experimental verification of the operation principle were fabricated in silica on silicon by a recently reported technique.[17] Advantages of this novel OADM with respect to OADMs based on TBGs are discussed.

2. Theoretical Analysis

Coupled-mode theory is widely used in the analysis of Bragg gratings.[15] Some basic results are summarized here as an aid to understanding the operation of the antisymmetric waveguide Bragg grating as a mode converter. At the Bragg condition the maximum re-

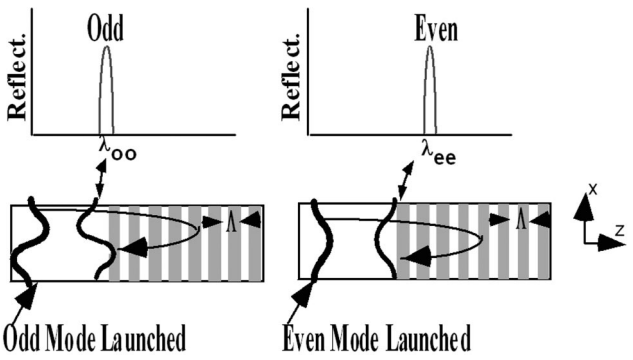


Fig. 1. Standard, untilted Bragg grating.

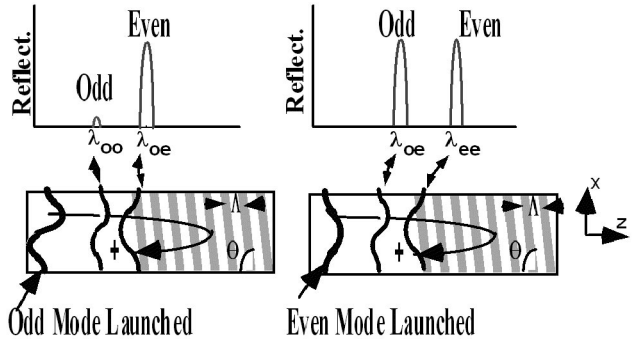


Fig. 2. Tilted Bragg grating.

flection from mode a to mode b is given by

$$R_{ab} = |r_{ab}|^2 = [\tanh(Kac_{ab}L)]^2, \tag{1}$$

where L is the grating length. Kac_{ab}, the coupling constant between the two waveguide modes a and b, is

$$Kac_{ab} = \frac{\pi}{\lambda}\,\Delta n \eta_{ab}, \tag{2}$$

where λ is the wavelength, Δn is the index modulation, and η_{ab} is the overlap integral between modes, given by[15]

$$\eta_{ab} = \frac{\iint e_a^*(x, y)\zeta(x, y)e_b(x, y)\mathrm{d}x\mathrm{d}y}{\left[\iint e_a^*(x, y)e_a(x, y)\mathrm{d}x\mathrm{d}y \iint e_b^*(x, y)e_b(x, y)\mathrm{d}x\mathrm{d}y\right]^{1/2}}, \tag{3}$$

where $\zeta(x, y)$ describes the profile of the index perturbation in the plane perpendicular to the guiding direction and $e_a(x, y)$ and $e_b(x, y)$ are the field amplitude profiles of modes a and b, respectively, propagating in the z direction.

The overlap integral indicates that, depending on $\zeta(x, y)$, some types of reflection may be increased while others are minimized. In a channel waveguide with two lateral modes (x direction) but only one vertical mode (y direction), the mode profiles may have either even or odd symmetry laterally across the waveguide. Standard Bragg grating with a uniform index profile, $\zeta(x, y) = 1$, written on that waveguide produce coupling only between modes that have the same profile ($a = b$), as shown in Fig. 1. However, because of fabrication constraints the perturbation profile is frequently not uniform along the vertical axis, and this can produce undesired coupling to cladding modes.

TBGs (Fig. 2) have the following index-perturbation profile[6,18]:

$$\zeta(x, y) = \exp\left[\frac{i2\pi x \tan(\theta)}{\Lambda}\right]F(y), \tag{4}$$

where θ is the grating tilt angle, Λ is the grating period in the propagation direction, and $F(y)$ is a function that represents variations of the grating in the vertical direction. $F(y)$ varies greatly, depending on the method of fabrication of the grating. For example, etched gratings do not usually extend through the waveguide height, and their index modulation changes as a function of depth. As an approximation to model an etched grating, $F(y)$ is assumed to be $\sim$1, with slow changes in the etched region, and $\sim$0 outside this region. To prevent undesired coupling between vertical modes owing to the asymmetric shape of $F(y)$, the waveguide is designed to be single mode in the vertical direction. In the lateral direction, because of the linearly varying phase across the waveguide, mode-converting reflections between forward-propagating modes and backward-propagating modes that are orthogonal ($a \neq b$) are possible. There is an optimum angle that maximizes the mode conversion. However, reflections between forward- and backward-propagating modes of the same profile ($a = b$) are still produced in various strengths at different wavelengths.[5,7] Figure 2 illustrates the predicted reflectivity of a TBG when even or odd modes are launched. The tilt of the grating is close to the angle that minimizes the odd–odd reflection (optimum).[5] It was predicted theoretically and demonstrated exper-

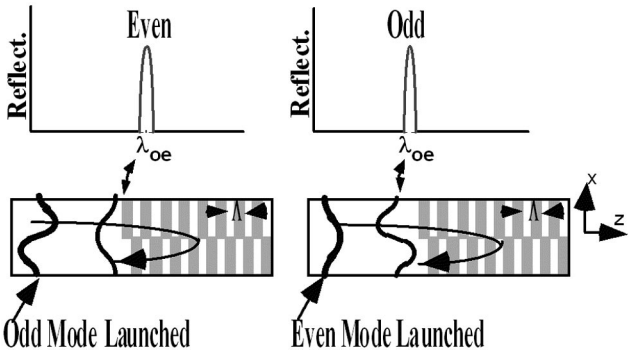


Fig. 3. Antisymmetric grating.

imentally[5,6] that there is no angle that minimizes the even–even reflection without drastically reducing the strength of the desired reflection with mode conversion. The effect of this unwanted even–even reflection can be minimized by choice of the proper input and outports; however, this reflection still produces noise and cross talk and places stringent requirements on the performance of the Y branch.

To obtain zero reflection between similar modes at all wavelengths, i.e., to avoid the undesired reflections produced by the TBGs, the overlap integral between similar modes ($a = b$) must be zero while the overlap integral of dissimilar modes is maximized;

$$\int\int \zeta(x, y)|e_{a=b}(x, y)|\mathrm{d}x\mathrm{d}y = 0. \tag{5}$$

Several solutions can satisfy Eq. (5). In a two-mode waveguide an antisymmetric index-modulation profile along the lateral axis will prohibit reflections without mode conversion. A simple approach to obtaining the desired response is shown in Fig. 3. The two-mode waveguide has a standard Bragg grating with an index modulation of periodicity

$$\Lambda = \lambda_{oe}/(n_e + n_o), \tag{6}$$

where λ_{oe} is the wavelength on Bragg condition for the reflection with mode conversion and n_e and n_o are the effective indices of the even and odd modes, respectively, at λ_{oe}. However, the grating is antisymmetric, equivalent to a $\Lambda/2$ longitudinal shift at the lateral center of the waveguide. Inside the waveguide, this antisymmetry in the index-modulation profile produces a π phase shift between left and right components of the modes, which can be represented by

$$\zeta(x, y) = \mathrm{sign}(x)F(y), \tag{7}$$

where x takes the value 0 at the center of the waveguide.

Figure 3 shows the reflection of the antisymmetric grating predicted by coupled-mode theory where even or odd modes are launched. The antisymmetric grating shows only the desired reflection peak, which represents the mode-conversion coupling between forward- and backward-propagating modes with orthogonal profiles.

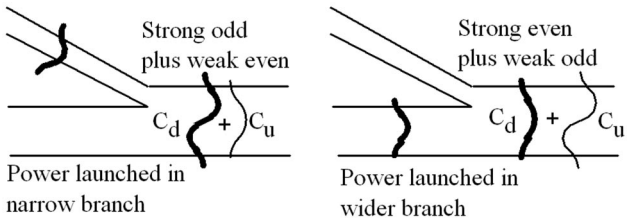


Fig. 4. Asymmetric Y-branch coupler.

Application of this type of grating to an OADM requires a coupler that can direct even and odd modes to different ports. Asymmetric Y branches[19] provide this type of operation, as shown in Fig. 4. In the figure, C_d and C_u represent the fraction of the input power coupled to the desired and undesired modes, respectively, of the two-mode waveguide. In an ideal condition without losses, $C_d = 1$ and $C_u = 0$. Using a conventional, symmetric Y branch will cause both modes to be equally excited ($C_d = C_u$) in the two-mode region. Owing to the characteristics of the antisymmetric waveguide grating, both modes will be reflected at the same Bragg wavelength. However, only half of the power will then be coupled out of the drop port, with the other half backreflected to the input port. This will produce unacceptable excess loss and, potentially, noise.

By contrast, when an asymmetric Y branch is used, ideally only the odd or even mode is excited in the two-mode waveguide ($C_d \sim 1$). Because of fabrication imperfections, a small amount of the undesired mode is also excited ($C_u > 0$). The parameter, mode cross talk, that describes the performance of the asymmetric Y branch is defined as

$$-10\log(C_d/C_u). \tag{8}$$

The mode cross talk can be minimized when the convergence of the Y branch to the waist is slow and when the asymmetry parameter, defined as the ratio between the widths of the wide and the narrow branches, is high.[5–20]

3. Design and Fabrication of the OADM

The design of an OADM, based on null couplers and a TBG, was explained in detail in Ref. 5. The conventional terminology for the device's four ports is used here for comparison purposes. It will be demonstrated that OADMs based on antisymmetric waveguide gratings do not need to follow this terminology, thus giving rise to increased flexibility in the device design. The prototype presented here was fabricated by use of silica-on-silicon waveguides and a previously reported technology.[17] For this prototype, the parameters for the refractive indices for the core (1.46) and the cladding ($\sim$1.4457), the waveguide height (1.6 μm), and the grating mesa height (400 nm) were used.

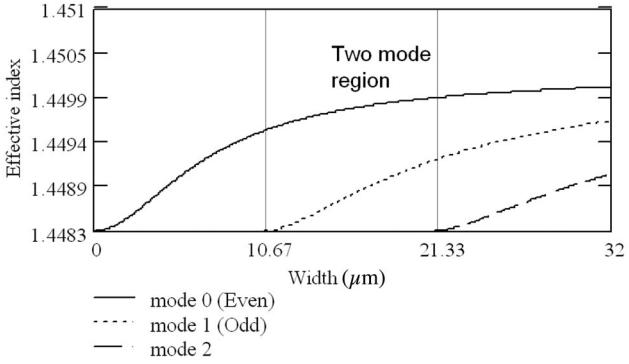


Fig. 5. Regions for one- and two-mode operation.

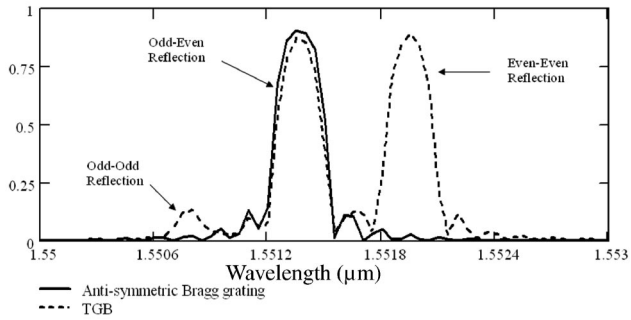


Fig. 6. Comparison of antisymmetric and tilted Bragg gratings.

A. Design

The cross talk of asymmetric Y branches was simulated by the beam propagation method. The structure consists of two single-mode waveguide branches that are initially separated by 125 μm and converge to a waist after a length of 8 mm. Results of the simulation show that cross talk of <20 dB can be obtained with an asymmetry parameter of ~1.5. Lower cross talk requires increasing the length or increasing the asymmetry parameter.

The effective-index method was used to determine the waveguide widths that allow one or two modes at 1.55 μm, as shown in Fig. 5. The waveguide height allows only one mode in the vertical direction. The widths of the branches need to be chosen to result in single-mode waveguides. They also must have an asymmetry parameter close to 1.5 to provide the desired cross talk. The waist should be a two-mode waveguide. The widths of the two branches and the waist were chosen to be 5.6, 8.4, and 14 μm, respectively. While it meets the design requirements, the device operates well away from the transition points from one to two modes and from two to three modes.

The grating period of ~0.530 μm for a Bragg wavelength of 1550 nm was calculated from Eq. (6) and the effective indices for the design widths. Etched grating were fabricated with a mesa height of 400 nm, as previously reported.[17] For these gratings the index modulation (Δn) for an equivalent grating with a uniform profile in the Y direction was computed as $\Delta n \sim 4 \times 10^{-4}$. The mode profiles were solved with both the effective-index method and the beam propagation method. These mode profiles were used in Eq. (3), yielding an overlap integral of ~0.5. Using Eq. (2), we obtained the coupling strength of the grating as $Kac_{eo} \sim 400\ \mathrm{m}^{-1}$. Reflections of the antisymmetric grating are compared in Fig. 6 with those of a TBG. Here, identical waveguides and grating strengths with the designed dimensions are used for 5 mm long gratings. Although the TBG shows three reflection peaks as expected, the antisymmetric grating permits only the desired reflection with mode conversion. Defects in the grating, such as having the point of the $\Lambda/2$ phase shift offset from the lateral center of the waveguide, would produce reflections without mode conversion. The wavelengths for these undesired reflections would be similar to those produced by the TBG (odd–odd and even–even).

B. Prototype Fabrication

Two types of device were fabricated. The first one (sample A) corresponds to the OADM. It consists of a two-sided asymmetric Y branch that converges to a waist, as shown in Fig. 7. The antisymmetric grating consists of mesas etched into the waist and filled with cladding material, and it operates in the first grating order corresponding to a grating period of ~530 nm. The length of the grating is 4.2 mm. The second sample (sample B) has waveguide and grating dimensions similar to those of sample A; however, it has only one asymmetric Y branch.

4. Characterization of the OADM

The experimental verification of the OADM requires measurements of the transmission and reflection spectra when either the even or the odd mode is excited. The effective index for the odd mode is lower than for the even mode. Therefore reflection peaks at different wavelengths when one is launching even or odd modes will indicate coupling without mode conversion. Similar Bragg conditions for the reflection peaks will indicate mode conversion between even and odd modes. Reflections without mode conversion produce cross talk in the drop port and backreflection in the input port. Before measurement of those spectra, a measurement of the asymmetric Y branch performance is necessary to ensure that it is providing the desired mode cross talk.

A. Y-Branch Performance as a Mode Splitter

The performance of the asymmetric Y branch was evaluated by use of both samples A and B. Sample B has the two-mode waist as the output waveguide. It was used to assess qualitatively the ability of the Y branch to excite either the even or the odd mode of the waist exclusively. Figure 8(a) shows the measured mode profile of the device when the power is launched in the wider branch. Figure 8(b) shows the measured mode profile when the power is launched in the narrow branch. These figures show that the Y branch is functioning properly, exciting primarily either the even or the odd mode of the waist, depending on the port used to input the power.

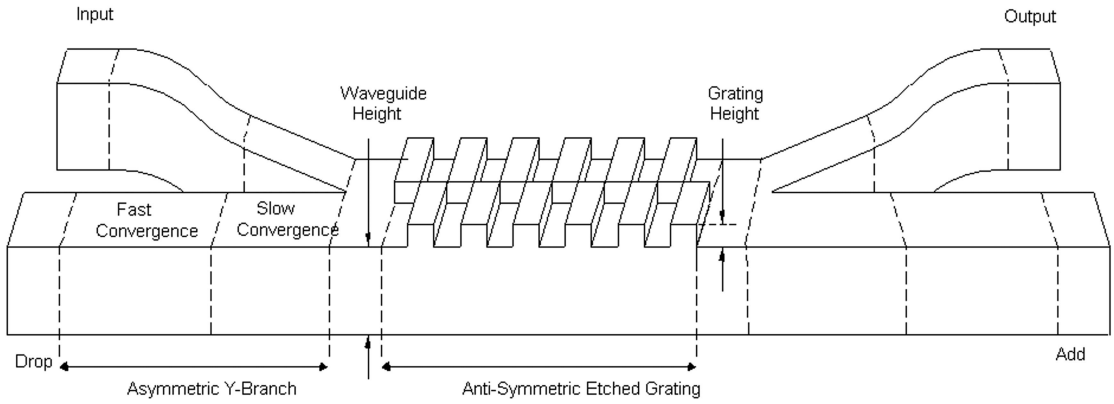


Fig. 7. Schematic of the OADM with an antisymmetric grating.

Sample A, which has Y branches on both sides of the two-mode waist, was used to measure the mode cross talk. To illustrate the procedure, consider a normalized power of 1 launched in narrow branch as shown in Fig. 4(a). It is assumed that there are no propagation losses. After the first Y branch, the desired and undesired modes have powers of C_d and C_u, respectively. Both modes couple to the second Y branch, producing $C_d^2 + C_u^2$ (power) at the narrow port and $2C_dC_u$ (power) at the wide port. From power measurement at both output ports the values of C_d and C_u and the mode cross talk can be calculated. A similar procedure can be used when the power is launched in the wider branch, as shown in Fig. 4(b).

Results of those measurements at wavelengths off Bragg condition are shown in Fig. 9. In the figure, lighter curves represent the power measured at the wider branch (dotted curve) and at the narrow branch (solid curve) when the input power is launched at the opposite wider branch. Similarly, darker curves represent the power measured at the narrow branch (dotted curve) and at the wider branch (solid curve) when the input power is launched at the opposite narrow branch. Using the procedure described in Section 2, we estimated the average mode cross talk per Y branch -23 dB.

B. Transmission and Reflection Spectra

Figure 10 shows the setup for characterization of the OADM's performance. Reflection and transmission spectra were measured with an erbium-doped fiber amplifier (EDFA) as an amplified spontaneous emission (ASE) source and an optical spectrum analyzer (OSA) with a resolution of 0.06 nm. A polarization controller permitted characterization of both TE and TM performance. A fiber array was used to couple light into and out of the device. After measurements, the spectra were normalized by use of the erbium-doped fiber-amplifier's amplified spontaneous emission profile. Figure 7 shows the conventional terminology used to follow the OADM ports. The input and drop ports are the narrow and wider branches, respectively, of the first Y branch. The output and add ports are the narrow and wider branches, respectively, of the second Y branch.

When TE power is launched to the input port, the odd mode of the waist is excited, as shown in Fig. 4(a). The odd mode on Bragg condition (1551.35 nm) is

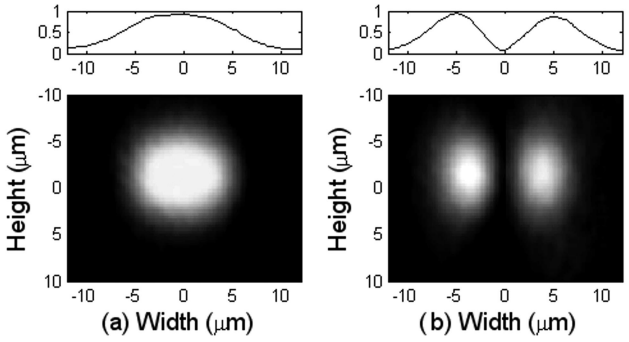


Fig. 8. Measured mode profiles for the (a) even and (b) odd modes.

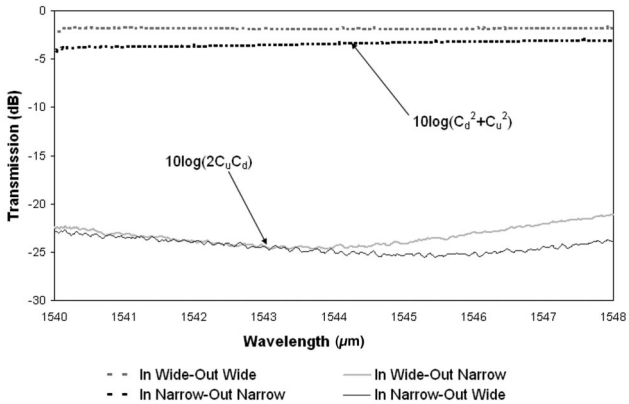


Fig. 9. Cross talk for two Y branches.

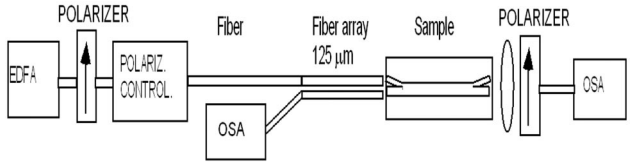


Fig. 10. Setup for transmission and reflection measurements.

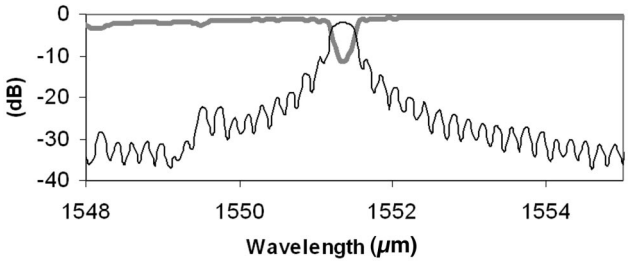


Fig. 11. Power launched in the narrower branch (input port). TE reflection (darker curve) measured in the drop port. TE transmission measured at the output port (lighter curve).

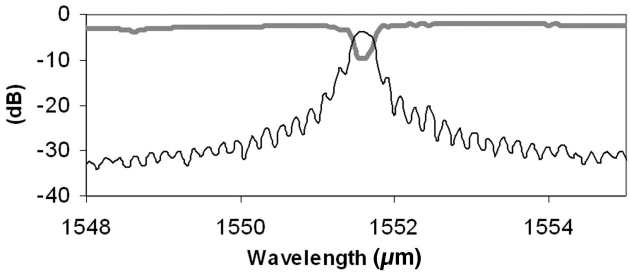


Fig. 13. Power launched in the narrower branch (input port). TM reflection measured (darker curve) in the drop port. TM transmission measured at the output port (lighter curve).

reflected as an even mode and coupled to the wider branch (drop port). The wavelengths off Bragg condition propagate through the waist and couple to the output port. The relevant transmission (output port) and reflection (drop port) spectra are shown in Fig. 11.

OADMs based on antisymmetric Bragg gratings do not need to follow the conventional port terminology. For this type of OADM the ports can be interchangeably used to add or drop. When TE power is launched in the drop port, even modes are excited. The even mode on Bragg condition (1551.35 nm) is reflected with mode conversion and coupled to the narrow input branch, which becomes the new drop port. The reflection spectrum at this port is shown in Fig. 12 by the darker curve. The wavelengths off Bragg condition travel to the other Y branch and couple to the add port. The transmission (TE) at the output is shown by lighter curve.

Similarly, the transmission and reflection spectra were measured for TM modes, as shown in Figs. 13 and 14. As can be seen, for each polarization the measured reflection spectra are identical; i.e., there is no dependence on the input port used. There is a strong reflection at the Bragg condition [Eq. (6)], which relates to the coupling between orthogonal modes. A uniform Bragg grating would produce two additional peaks (dips) for the even–even and the odd–odd reflection (transmission) with the wavelength separation similar to that shown in Fig. 6 for a TBG.

A shift in the Bragg wavelength owing to the polarization dependence was measured as 0.25 mm. The polarization dependence is due to the waveguide asymmetry and to the strain-induced waveguide birefringence. The first polarization dependent component was expected from the design and can be improved by reducing the width–height asymmetry. The second is a well-known problem of the silica-on-silicon platform that can be overcome by various fabrication methods that yield essentially polarization-independent gratings.[21]

From the measurements and Eq. (1), the coupling coefficient of $Kac_{eo} = 400\ \mathrm{m}^{-1}$ is obtained. The overlap integral computed from the measured mode profiles and Eq. (3) is 0.48. Using Eq. (2), we obtained an index modulation of 4.2×10^{-4}. All these three parameters calculated from measured characteristics are in good agreement with the parameters predicted theoretically.

5. Operation and Advantages of the Designed OADM

The basic operation of similar devices that use TBGs was explained previously.[2–6] As shown in Fig. 15, from the input port (narrower branch) several wavelength-division multiplexing (WDM) channels excite the odd mode of the waist. The channel to be dropped is on Bragg condition, and it is reflected as an even mode by the antisymmetric grating. It is then coupled to the drop port (wider branch). The other channels, which are out of Bragg condition, are transmitted to the second Y branch, where they are coupled to the output port. From the add port one channel can be coupled to a backward-traveling even mode and reflected by the grating as an odd mode that is coupled to the output port.

The use of the antisymmetric waveguide grating in place of the previously demonstrated TBG prevents

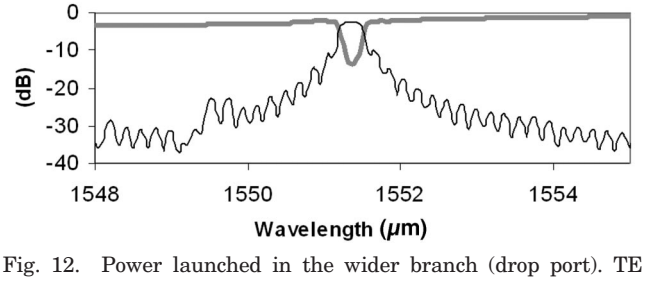


Fig. 12. Power launched in the wider branch (drop port). TE reflection (darker curve) measured in the input port. TE transmission measured at the add port (lighter curve).

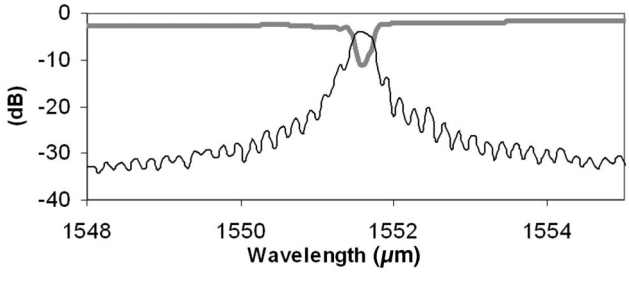


Fig. 14. Power launched in the wider branch (drop port). TM reflection (darker-curve) measured in the input port. TM transmission (lighter curve) measured at the add port.

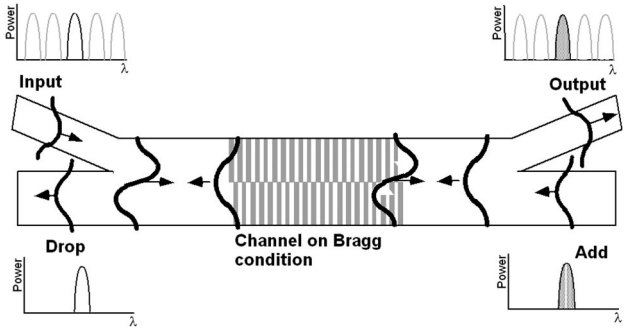


Fig. 15. Schematic showing the OADM structure and method of operation.

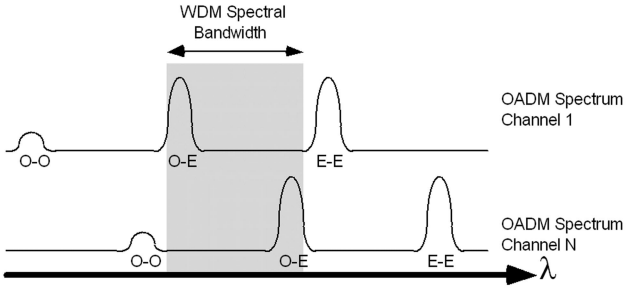


Fig. 16. Noise-free bandwidth limits the number of channels to be transmitted in an OADM-based on a TBG.

reflections without mode conversion. This improves performance in terms of cross talk and signal-to-noise ratio. In the optimum configuration[5] the cross talk at the drop port of the OADM based on a TBG depends on the performance of the asymmetric Y branch, as previously explained.[5,6] For example, a nonideal Y branch with mode cross talk of −20 dB (1%) would produce approximately the same value for the cross talk, as nearly all that power launched in the even mode would be reflected to a backward-traveling even mode at λ_{ec} and routed out through the drop port.

In the OADM described here, the same nonideal Y branch will not produce that cross talk. The 1% of the power coupled to the undesired even mode would be reflected at the same wavelength as an odd mode. It would then be routed out the input port as backreflection. Therefore no cross talk is produced because both desired and undesired modes are subject to the same Bragg condition as shown in Eq. (6). In both types of OADM, however, defects on the Y branch can increase backreflection to the input port. Reflected light coupled back to the launch port should have the same spectral shape as the reflection out the drop port but reduced by an amount equal to the mode coupling in the asymmetric Y-branch (~23 dB). The reduced mode-splitter performance requirements relax the asymmetric Y-branch fabrication tolerances and permit reduction in its length. Shorter Y branches improve the integratability of the OADM.

The antisymmetric gratings also add versatility to the null coupler OADM. Because of the exclusive reflection with mode conversion, the order of the ports can be exchanged. The input (or drop) port can be either the wide or the narrow branch without affecting the performance of the device. This characteristic provides more flexibility for integrating these OADMs into more-complex structures. By contrast, a TGB has to follow rigorously the conventional port nomenclature. Because there is always a strong even–even reflection, power from the input port should not excite the even mode of the waist. A configuration in which the wider branch is the input port would produce extremely high cross talk between nonadjacent channels (~0 dB).

Another advantage of the OADM based on antisymmetric gratings is the increase of the operational range that can be used to add or drop WDM channels.[22] OADMs based on a TBG working at the optimum angle would not add noise in the interval of wavelengths between the even–even and odd–odd reflection.[22] The bandwidth free of spurious reflections, or noise-free bandwidth, can be obtained as

$$\Delta\lambda_{\mathrm{fn}} = \frac{\lambda_{ee} - \lambda_{oo}}{2}, \tag{9}$$

where λ_{ee} and λ_{oo} are the Bragg wavelength for even–even and odd–odd reflection, respectively. Therefore, to prevent spurious reflections that would reduce the optical signal-to-noise ratio of the dropped channel, the WDM spectral bandwidth of the total number of channels ($\Delta\lambda$) should be lower than the bandwidth free of noise ($\Delta\lambda_{\mathrm{fn}} > \Delta\lambda$), as shown in Fig. 16. OADMs based on TBGs have a noise-free bandwidth that allows for few WDM channels.[22] By contrast, OADMs based on antisymmetric gratings have noise-free bandwidths that can cover all WDM bands because there is only one reflection at λ_{oe}.

6. Summary

We have designed and experimentally demonstrated a novel optical add–drop multiplexer based on antisymmetric waveguide Bragg gratings and asymmetric Y branches. Cross-talk improvement in comparison with similar OADMs based on TBGs was demonstrated. A potential for the reduction in the size of the OADM owing to shorter Y branches was discussed. Additional advantages such as versatility in use of the ports and a significant increase in the operational range of the OADM were presented. Our OADM prototype has a reflectivity peak of ~90% because of the short grating length (5 mm). From the calculation of the coupling constant, a reflectivity of 99.9% is estimated for lengths of ~1 cm. We are confident that the advantages provided by the antisymmetric waveguide Bragg grating in terms of performance, compactness, and scalability can be applied to other devices such as dispersion compensators, optical correlators, and resonators.

This research is supported by the National Science Foundation under grant ITR 0325979.

References

1. A. V. Tran, W. D. Zhong, R. C. Tucker, and R. Lauder, "Optical add–drop multiplexers with low crosstalk," IEEE Photon. Technol. Lett. **13,** 582–584 (2001).
2. A. S. Kewitsch, G. A. Rakuljic, P. A. Willems, and A. Yariv, "All-fiber zero-insertion-loss add–drop filter for wavelength-division multiplexing," Opt. Lett. **23,** 106–108 (1998).
3. C. K. Madsen, T. A. Strasser, M. A. Milbrodt, C. H. Henry, A. J. Bruce, and J. Demarco, "Planar waveguide add/drop filter employing a mode converting grating in an adiabatic coupler," in *Integrated Photonics Research,* Vol. 4 of OSA 1998. Technical Digest Series (Optical Society of America, 1998), pp. 102–104.
4. D. F. Geraghty, D. Provenzano, M. M. Morrell, S. Honkanen, A. Yariv, and N. Peyghambariam, "Ion-exchanged waveguide add/drop filter," Electron Lett. **37,** 829–831 (2001).
5. C. Riziotis and M. N. Zervas, "Design considerations in optical add/drop multiplexers based on grating-assisted null couplers," IEEE J. Lightwave Technol. **19,** 92–104 (2001).
6. J. M. Castro, D. F. Geraghty, B. West, and S. Honkanen, "Fabrication and comprehensive modeling of ion-exchanged Bragg optical add/drop multiplexers," Appl. Opt. **43,** 6166–6173 (2004).
7. E. Marin, R. Ghosh, J.-P. Meunier, X. Dexhelet, and S. Lacroix, "Bragg gratings in 2 $\times$ 2 symmetric fused fiber couplers: influence of the tilt on the wavelength response," IEEE Photon. Technol. Lett. **11,** 1434–1436 (1999).
8. T. Erdogan, "Optical add–drop multiplexer based on an asymmetric Bragg coupler," Opt. Commun. **157,** 249–267 (1998).
9. G. Perrone, M. Laurenzano, and I. Montrosset, "Design and feasibility analysis of an innovative integrated grating-assisted add–drop multiplexer," J. Lighwave Technol. **19,** 1943–1948 (2001).
10. M. Åslund, J. Canning, L. Poladian, C. M. de Sterke, and A. Judge, "Antisymmetric grating coupler: experimental results," Appl. Opt. **42,** 6578–6583 (2003).
11. S. Tomljenovic-Hanic and J. D. Love, "Planar waveguide add/drop wavelength filters based on segmented gratings," Microwave Opt. Technol. Lett. **37,** 163–165 (2003).
12. J. M. Castro, A. Sato, and D. F. Geraghty, "Waveguide mode conversion using anti-symmetric gratings," in *Optical Fiber Communication Conference (OFC)* (Optical Society of America, 2005), paper 0ME31.
13. J. M. Castro, D. F. Geragthy, C. M. Greiner, D. Iazikov, and T. W. Mossberg, "Novel antisymmetric Bragg gratings for mode conversion," in *Integrated Photonics Research,* 2005 OSA Topical Meeting Digest Series (Optical Society of America, 2005), paper ITuF7.
14. J. M. Castro, D. F. Geragthy, S. Honkanen, C. M. Greiner, D. Iazikov, and T. W. Mossberg, "Demonstration of mode conversion using anti-symmetric waveguide Bragg gratings," Opt. Express **13,** 4180–4184 (2005).
15. R. Kashyap, *Fiber Bragg Gratings* (Academic, 1999).
16. P. L. Ho and Y. Y. Lu, "A bidirectional beam propagation method for periodic waveguides," IEEE Photon. Technol. Lett. **14,** 325–327 (2002).
17. C. Greiner, T. W. Mossberg, and D. Iazikov, "Bandpass engineering of lithographically scribed channel-waveguide Bragg gratings," Opt. Lett. **29,** 806–808 (2004).
18. T. Erdogan and J. E. Sipe, "Tilted fiber phase gratings," J. Opt. Soc. Am. A **13,** 296–313 (1996).
19. W. K. Burns and F. Milton, "Mode conversion in planar-dielectric separating waveguides," IEEE J. Quantum Electron. **11,** 32–39 (1975).
20. C. P. Hussell, R. V. Ramaswamy, and R. Srivastava, "Wavelength and polarization insensitive 3 dB cross-coupler power dividers by ion exchange in glass," Appl. Phys. Lett. **56,** 2381–2382 (1990).
21. R. Adar, C. H. Henry, R. H. Kistler, and R. F. Kazarinov, "Polarization independent narrow band Bragg reflection gratings made with silica-on-silicon waveguides," Appl. Phys. Lett. **60,** 1779–1781 (1992).
22. J. M. Castro and D. F. Geraghty, "Optimization of optical add drop multiplexers based on grating-assisted null couplers," Opt. Eng. **44,** 095002 (2005).